CHEMISTRY
A EUROPEAN JOURNAL

DOI: 10.1002/chem.200800381

# Hetero-Seeding and Solid Mixture to Obtain New Crystalline Forms

**Dario Braga,*[a] Fabrizia Grepioni,[a] Lucia Maini,*[a] Marco Polito,[a] Katia Rubini,[a] Michele R. Chierotti,[b] and Roberto Gobetto*[b]**

**Abstract:** *Para*-methyl benzyl alcohol (*p*-MeBA II) and *para*-chloro benzyl alcohol (*p*-ClBA) are quasi-isostructural and share the same hydrogen-bond patterns, but their crystals are not isomorphous. No new polymorphs could be obtained by conventional polymorph screening based on different solvents and different crystallization conditions. Formation of a new polymorph of *p*-MeBA named *p*-MeBA I, isomorphous with the crystal of *p*-ClBA, was induced by hetero-seeding with a small quantity of powdered *p*-ClBA added to a supersaturated solution of *p*-MeBA in hexane, while seeding of *p*-ClBA with *p*-MeBA II failed to give a new phase of *p*-ClBA isomorphous with known crystalline *p*-MeBA II. Mixed crystals of *p*-MeBA and *p*-ClBA were also prepared with different *p*-MeBA/*p*-ClBA ratios to understand the role of the different functional groups in the crystal structure. Crystal phases were characterized by combined use of single-crystal and powder X-ray diffraction, differential scanning calorimetry, and solid-state NMR spectroscopy.

**Keywords:** crystal engineering · differential scanning calorimetry · hetero-seeding · hydrogen bonds · NMR spectroscopy · polymorphism

## Introduction

Polymorphism, the existence of more than one crystal structure for the same molecule or molecular aggregate (salt, co-crystal, solvate),[1–3] is a hot topic in solid-state chemistry research. The phenomenon of crystal polymorphism, with its still ample degree of unpredictability, represents a major challenge to our ambitions of crystal design and rational control of crystal nucleation and growth.[4] Since different crystal forms can differ in their physical and chemical behaviors (solubility, bioavailability, thermal stability, hardness, processability etc.), the understanding of the conditions that lead to the interconversion of known crystal phases or to the formation of new ones is of paramount importance when dealing with active pharmaceutical ingredients or other molecular materials (agrochemicals, explosives, pigments, etc).

To attain polymorph selection, the processes of nucleation, growth, and crystallization have to be mastered. As a matter of fact, the experimental investigation of crystal polymorphism is still mainly based on systematic (manual or automatic) solvent and thermal screenings.[5] However, the recent literature proposes new methodologies to explore the formation of new phases, such as the use of polymer heteronuclei,[6] additives,[7–9] solvent-free reactions,[10] mechanical-grinding processes,[11–13] supercritical fluids,[14,15] and high-pressure conditions.[16–18] The utilization of hetero-seeds to induce the desired form has also been used successfully.[19,20] Usually, the hetero-seed is a crystalline sample formed by molecules that possess almost the same structure as the compound of interest. The difference may be due to a substituent or, as in the case of salts, a different counterion. It is known that chlorine and methyl groups have similar van der Waals volumes (21 and 19 Å$^3$ for Cl and Me, respectively), so it should be possible for molecules containing chlorine atoms or methyl groups in chemically equivalent sites to have the same crystal structure according to the Kitaigorodskii principle of close packing,[21,22] although their different inductive effect might play an active role in modifying the

[a] Prof. D. Braga, Prof. F. Grepioni, Dr. L. Maini, Dr. M. Polito, K. Rubini
Dipartimento di Chimica "G. Ciamician"
Università degli studi di Bologna
Via Selmi 2, 40126 Bologna (Italy)
Fax (+39) 051-209-9456
E-mail: dario.braga@unibo.it
l.maini@unibo.it

[b] Dr. M. R. Chierotti, Prof. R. Gobetto
Dipartimento di Chimica I.F.M., Università di Torino
Via P. Giuria 7, 10125 Torino (Italy)
Fax (+39) 011-670-7855
E-mail: Roberto.gobetto@unito.it

Supporting information for this article is available on the WWW under http://dx.doi.org/10.1002/chem.200800381.

stabilizing interactions.[23] Jones et al.[24] described the case of methyl and chlorine cyclopentanone derivatives that crystallize with different conformations, so that the methyl derivative is photoactive and undergoes dimerization upon UV irradiation, while the chlorine derivative is photostable; crystallization of the chlorine derivative in the presence of the methyl derivative leads to formation of a solid solution crystal, isomorphous with the photoactive crystal. The phenomenon by which in mixed crystals the molecular geometry of the minor component is forced to adopt the packing mode of the dominant second component was called "structural mimicry" by Sacconi et al.[25]

However, in a recent study, Motherwell et al.[26] argued that the formation of a Cl···Cl interaction[27] seemingly prevents the formation of isomorphic phases in isostructural Cl/Me molecules. The influence of Cl···Cl interactions in the crystal structural energy minimization is still under debate, and both geometric and energetic considerations have to be taken into account.[28–30]

Our purpose is to extend the use of the hetero-seeding method to induce new phases, focusing our attention on the pair *para*-methyl benzyl alcohol (*p*-MeBA) and *para*-chloro benzyl alcohol (*p*-ClBA). One crystal structure is known for each compound,[31–33] and they are not isomorphous, even though they are based on the same hydrogen-bond pattern and show similar packing structures (vide infra). In the following we report a full diffractometric, calorimetric, and spectroscopic investigation of the effect of hetero-molecular seeding on polymorph selection and on the preparation of mixed crystalline materials of various compositions by changing the *p*-MeBA/*p*-ClBA ratio.

## Results and Discussion

**Crystal structures of *para*-methyl benzyl alcohol and *para*-chloro benzyl alcohol and cross hetero-seeding**: The crystal structures of *para*-methyl benzyl alcohol (*p*-MeBA II) and *para*-chloro benzyl alcohol (*p*-ClBA) are not isomorphous. The structure of *p*-ClBA has been studied by Hashimoto[31,32] at different temperatures. The molecule crystallizes in a monoclinic system with space group $P2_1$ and one independent molecule ($Z=1$) in the asymmetric unit. The crystal structure is characterized by chains of OH···O hydrogen bonds extending along a $2_1$ axis. These chains run parallel to each other (see Figure 1) with an O···O distance of 2.746(4) Å at room temperature.

This phase is known to undergo a first-order phase transition at −37 °C.[31] The two phases adopt almost the same structure and are isomorphic. However, they differ in the orientation of the hydroxyl hydrogen atom with respect to the benzene ring shifting from the *cis* to the *trans* position at temperatures less than −37 °C, and in the O···O distance, which shows a small discontinuity (2.746(4) Å at room temperature, 2.741(3) Å at −33 °C; 2.752(2) Å at −140 °C) consistent with the slight change in the nature of the OH···O bond. No interactions are present between the chlorine atoms, because the distance between them is higher than the sum of the van der Waals radii.[27]

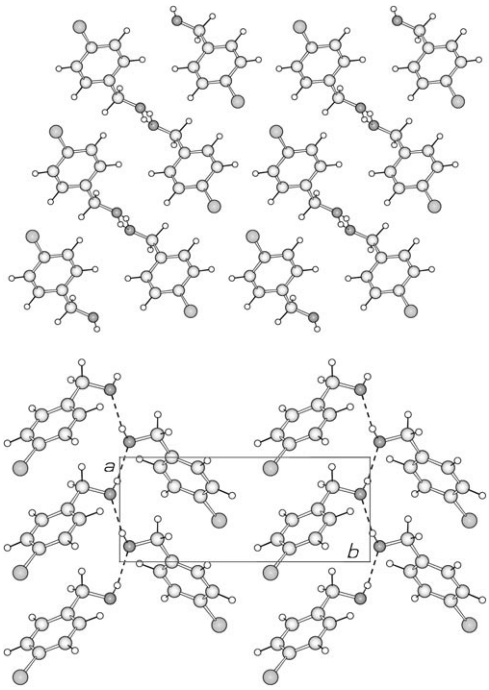


Figure 1. Crystal packing of *p*-ClBA, view along the *b* axis (top) and the *c* axis (bottom).

The *p*-MeBA II crystal also exhibits a phase transition to another crystal form, which resembles that of *p*-ClBA although they are not isomorphic.[33] The *p*-MeBA II crystal is monoclinic with space group $P2_1$ and three independent molecules ($Z=3$), denoted as molecules A, B, and C, in the asymmetric unit (see Figure 2).

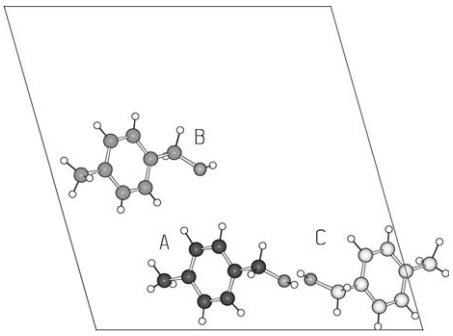


Figure 2. The three asymmetric molecules in the cell of *p*-MeBA II.

The B molecule forms infinite OH···O hydrogen bonded chains along the $2_1$ axes with an O···O distance of 2.746(4) Å at −30 °C, while the A and C molecules form other chains related by a pseudo $2_1$ axis along the *b* axis, with O···O distances of 2.724(4) and 2.749(5) Å at −30 °C (see Figure 3).

As in *p*-ClBA, the *p*-MeBA II crystal shows a first-order phase transition at −62 °C due to the shift of the hydroxyl

  

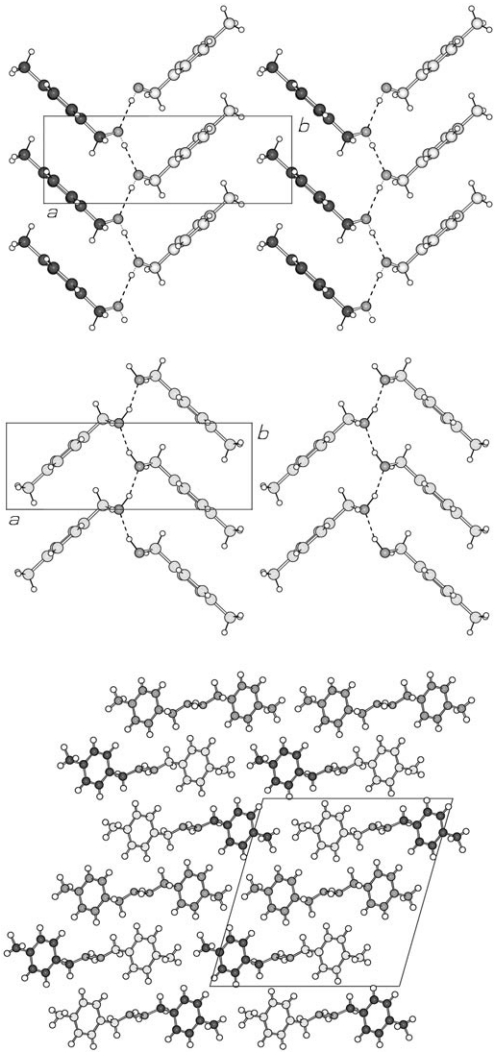


Figure 3. Crystal packing of *p*-MeBA II. View along the *c* axis of the chains formed by molecules A and C (top) and by molecule B (middle). View along the *c* axis (bottom).

hydrogen atoms from the *cis* to the *trans* position at low temperature. The main difference between the structure of *p*-ClBA and *p*-MeBA II is the position of the chains. Whereas in *p*-ClBA they all have the same orientation with respect to the *b*-axis, in *p*-MeBA II chain 1 and chain 2 have opposite directions with respect to the *b* axis.

A comparison of the measured and calculated powder diffraction patterns shows that the commercial products correspond to the respective room-temperature phases, albeit with severe problems of preferential orientation. The differential scanning calorimetry (DSC) heating traces of the commercial products show that melting takes place at 70.4 and 59.3 °C for *p*-ClBA and *p*-MeBA II, respectively.

Non-exhaustive polymorph screening was performed on the two compounds. *p*-ClBA and *p*-MeBA II were recrystallized from water, ethanol, acetone, ethyl-lactate, dioxane, hexane, toluene, nitromethane, THF, (*S*)-methylbutanol, glicole, and dicholoromethane. In all cases the obtained phase was the same as the starting compounds. Similarly, crystallization from supersaturated solutions of the compounds in hexane, quenching of the melt, and sublimation did not yield any new phases.

Since the two compounds are similar, but not isomorphic, we attempted to induce the crystallization of new phases by hetero-seeding. A small quantity of powder of *p*-ClBA was added to a supersaturated solution of *p*-MeBA in hexane before nucleation of the latter occurred. Powder diffraction patterns of the recovered precipitate showed significant differences from the known phase. To minimize preferential orientation effects, the diffraction patterns of the known phase (*p*-MeBA II) and that of the alleged new phase (hereafter *p*-MeBA I) were collected on a capillary stage and compared.

Figure 4 shows the comparison of the powder patterns of the two polymorphs. The profiles are similar, but *p*-MeBA II presents peaks at $2\theta = 6.2$, 9.8, 12.0, 20.8, and 21.7° that are missing in the profile of *p*-MeBA I. Single-crystal X-ray diffraction on *p*-MeBA I showed how the structure is isomorphous with that of *p*-ClBA (see Table 2). The small variations in the crystal packing account for the small differences in the calculated powder diffraction patterns of forms I and II.

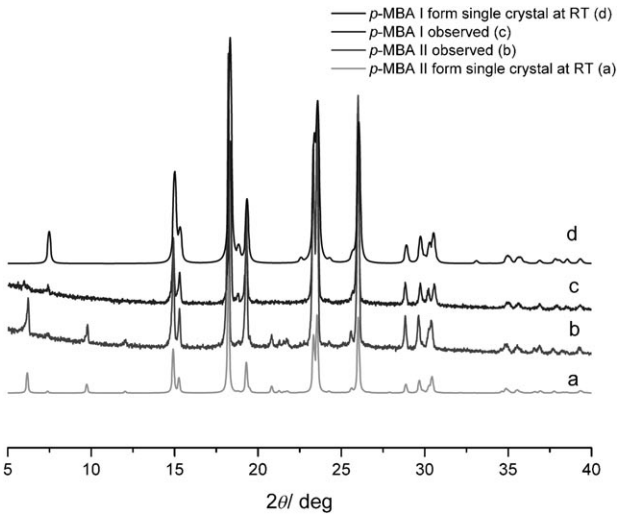


Figure 4. Comparison of the observed and calculated powder diffraction patterns of *p*-MeBA II (bottom) and *p*-MeBA I (top).

DSC traces of the two phases show only the endothermic peak of the melting at 58.0 °C ($\Delta H = 18.7\ kJ\,mol^{-1}$) for *p*-MeBA I and at 59.3 °C ($\Delta H = 18.8\ kJ\,mol^{-1}$) for *p*-MeBA II. A slurry experiment at room temperature (see the Experimental section) shows that, within a week, *p*-MeBA I converts into *p*-MeBA II, which is then the thermodynamically stable phase at room temperature. The new phase *p*-MeBA I was obtained also by seeding a supersaturated hexane solution with crystals of *p*-MeBA I.

DSC and slurry experiments suggest forms I and II constitute a monotropic system, in which form II is the thermody-

  

namically stable phase and form I is the metastable one. Attempts to obtain a new *p*-ClBA phase through the symmetrical process, that is, by addition of a small quantity of powder of *p*-MeBA II to a supersaturated solution of *p*-ClBA in hexane before nucleation, did not yield crystals isomorphous with *p*-MeBA II or any other new phase. All attempts led to crystals of *p*-ClBA.

It is worth noting that *p*-MeBA I and II possess different $Z$ values, with the higher value for the thermodynamically stable form ($Z=3$, compared with $Z=1$ of the metastable form). Structures with $Z>1$ have been discussed recently in the scientific community[34–37] and it is commonly accepted that the thermodynamically stable form should present the lower $Z$, although there is no experimental evidence[38] supporting this prediction, which our system appears to contradict.

**Solid-state NMR characterization**: Solid-state NMR (SSNMR) spectroscopy has emerged as an important technique for the characterization of crystalline solids,[39–41] of pharmaceutical compounds,[42] and in the field of polymorphism.[43,44] Since conformational differences can result in variations of internuclear distances and in the local electronic structure, SSNMR spectroscopy is an ideal and sensitive probe for characterizing this type of behavior and can provide information complementary to other structural analysis techniques, such as X-ray diffraction and calorimetric methods.

The NMR data for compounds *p*-ClBA, *p*-MeBA II as well as for the new phase *p*-MeBA I obtained as described above are summarized in Table 1, while $^{13}C$ CPMAS spectra

Table 1. $^{13}C$ CPMAS NMR data [ppm] for the compounds *p*-ClBA, *p*-MeBA II and *p*-MeBA I.

| | *p*-ClBA | *p*-MeBA II | *p*-MeBA I |
|---|---|---|---|
| aromatic Cq | 139.7 | 138.4 | 138.2 |
| | 137.5 br | | |
| aromatic CH | 129.6 | 129.4 | 129.1 |
| | 131.6 sh | | 130.8 sh |
| $CH_2$ | 62.8 | 63.5 | 63.7 |
| $CH_3$ | – | 20.6 | 20.6 |

are displayed in Figure 5. Since the crystal packing of the three compounds shows almost the same features (similar hydrogen-bond network and similar interatomic distances as described above), relatively small differences are present in the $^{13}C$ CPMAS spectra. However, the shifts of the aromatic carbon signals (around $\delta=150$–$100$ ppm; Figure 6) allow a distinction between samples and phases. The spectrum of *p*-ClBA is characterized by a peak at $\delta=129.6$ ppm with a shoulder at $\delta$131.6 ppm for the CH carbon atoms, and by two resonances at $\delta=139.7$ and at 137.5 ppm for the *C*–$CH_2OH$ and *C*–Cl quaternary carbon atoms, respectively. Since one molecule is present in the symmetric unit cell the shoulder at $\delta=131.6$ ppm arises from different local environments of the four protonated aromatic carbon atoms.

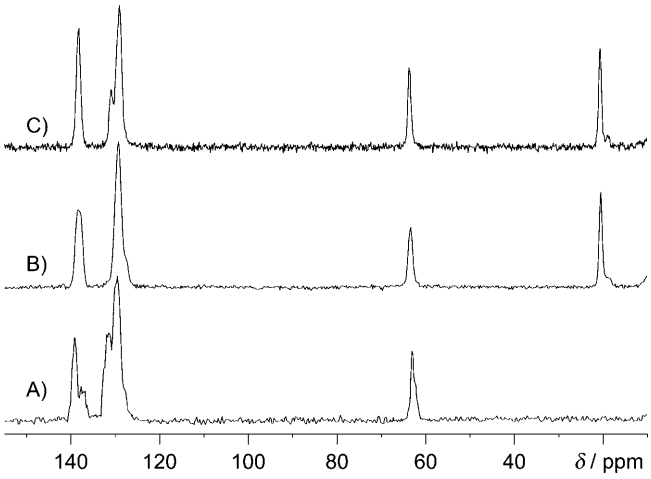


Figure 5. $^{13}C$ CPMAS NMR spectra for A) *p*-ClBA, B) *p*-MeBA II, and C) *p*-MeBA I.

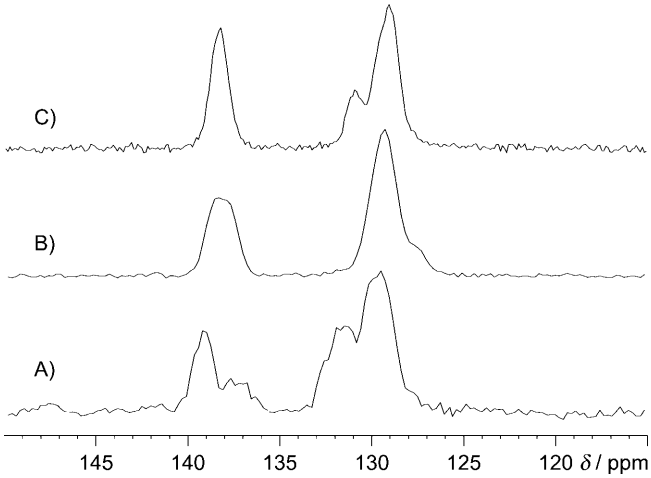


Figure 6. Aromatic region of the $^{13}C$ CPMAS NMR spectra for A) *p*-ClBA, B) *p*-MeBA II, and C) *p*-MeBA I.

Indeed, by careful inspection of the crystal structure, it is possible to detect a C–H···π contact[45] between a methylene hydrogen and an aromatic carbon atom ($C_7$–$H_6$···$C_5$ distance equal to 2.86 Å with H distance normalized to 1.08 Å), whereas the other three aromatic CH moieties are not influenced by any other weak interactions, thus justifying the signal intensity ratio of about 1:3.

Conversely, the $^{13}C$ spectrum of *p*-MeBA II shows only two sharp peaks in the aromatic region at $\delta=129.4$ and at 138.4 ppm, in agreement with negligible differences in the crystal structure of the three independent molecules. The high-frequency region of *p*-MeBA I is more similar to the *p*-ClBA spectrum than the *p*-MeBA II one. Indeed, for *p*-MeBA I, the presence of a shoulder at $\delta=130.8$ ppm attributed to the CH groups confirms the achievement of phase I, with a crystal packing and an asymmetry close to that of the *p*-ClBA compound. This is in agreement with the X-ray analysis, which shows a C–H···π interaction between the

  

methylene hydrogen and the aromatic carbon atom ($C_1$–$H_{1A}\cdots C_6$ distance equal to 2.85 Å with H distance normalized to 1.08 Å)

**Solid mixture experiments**: The availability of the new phase *p*-MeBA I and its isomorphism with the crystal phase *p*-ClBA prompted us to investigate the Me/Cl analogy. To explore to what extent the isomorphism between *p*-ClBA and *p*-MeBA I could be exploited, different molar mixtures of *p*-ClBA/*p*-MeBA were prepared. Crystalline solids were obtained by melting together *p*-ClBA and *p*-MeBA and then quenching the mixture with ice or liquid nitrogen. This procedure avoids the problems associated with the different solubilities of *p*-ClBA and *p*-MeBA in most common solvents. The two components, in the case of the quenching with ice, form phase I (*p*-ClBA or *p*-MeBA I) in all the different *p*-ClBA/*p*-MeBA ratios according to XRPD data. The melting points reported in Figure 7 were measured by DSC analysis.

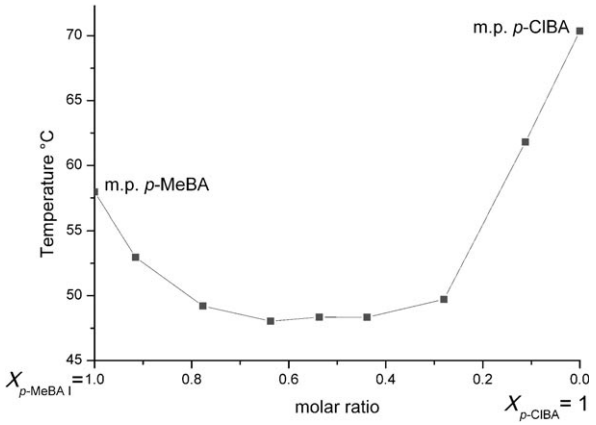


Figure 7. Melting points of solid solutions of *p*-ClBA and *p*-MeBA as phase I.

Conversely, in the case of quenching with liquid nitrogen, the mixture *p*-ClBA/*p*-MeBA behaves as a solid solution only up to a 50:50 ratio; its structure corresponds to that of phase I (*p*-ClBA or *p*-MeBA I), as shown in Figure 8.

The diffractogram of the mixture *p*-ClBA/*p*-MeBA 50:50 was indexed by DASH[46] with a monoclinic cell with parameters $a=12.198$, $b=4.958$, $c=5.959$ Å, $\beta=104.34°$ and $V=348$ Å$^3$, consistent with the parameters of form I. The disorder due to the presence of methyl groups or chlorine atoms leads principally to an increase of the $\beta$ angle from around 102° in the mono-component phase to around 104° in the solid solution.

Crystallization from solution of the mixture *p*-ClBA/*p*-MeBA 40:60 seeded with *p*-ClBA crystals allowed the formation of single crystals of the appropriate size for X-ray diffraction. The crystal structure, determined both at room temperature and low temperature (−123 °C), is isomorphic with that of *p*-ClBA, with cell parameters $a=12.159(1)$, $b=4.9749(7)$, $c=5.9592(9)$ Å, $\beta=103.75$ (1)° and $V=350.14(8)$ Å$^3$ at room temperature. As expected on the basis of powder indexation on the 50:50 mixture, the $\beta$ angle is close to 104°. It is worth noting that the hydroxyl hydrogen atom is in *cis* position with respect to the benzene ring in the crystal structure at room temperature, while it is in *trans* position at −123 °C (see Figure 9); therefore the mixed crystal undergoes the same phase transition at low temperature as observed for the pure crystals of *p*-ClBA and *p*-MeBA II.[31,33]

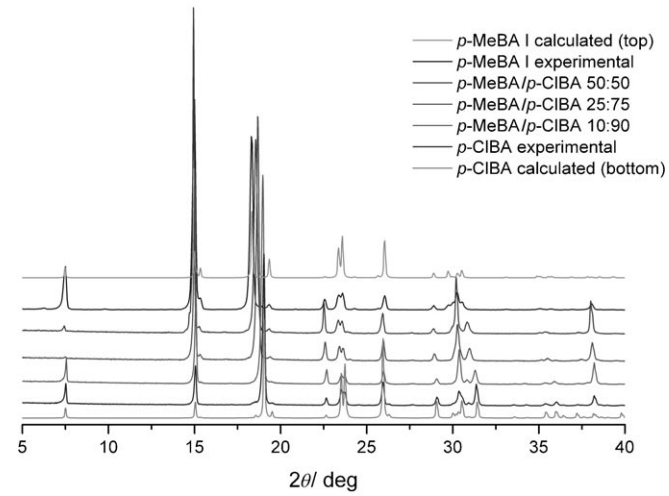


Figure 8. X-ray powder patterns (from bottom) of *p*-ClBA calculated and experimental, *p*-ClBA/*p*-MeBA in 10:90, 25:75, and 50:50 molar ratio and *p*-MeBA I (top) experimental and calculated.

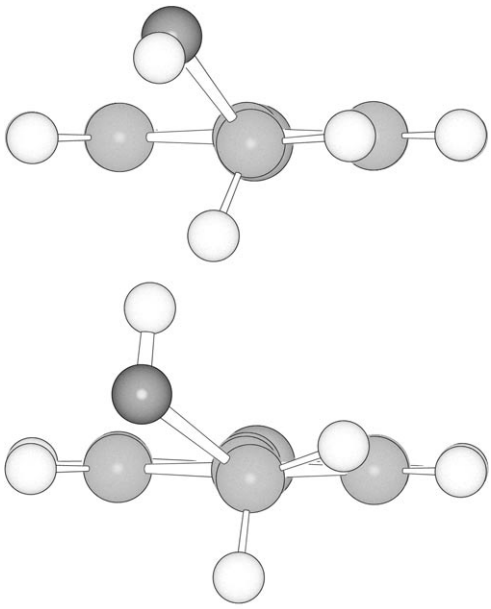

Figure 9. The orientation of the −OH group with respect to the benzene ring in the *p*-ClBA/*p*-MeBA 40:60 crystal at room temperature (top) and at −123 °C (bottom).

When the percentage of *p*-MeBA becomes higher (75% or 90%) the diffraction patterns are not consistent with either *p*-MeBA I or *p*-MeBA II phases, as shown in Figure 10.

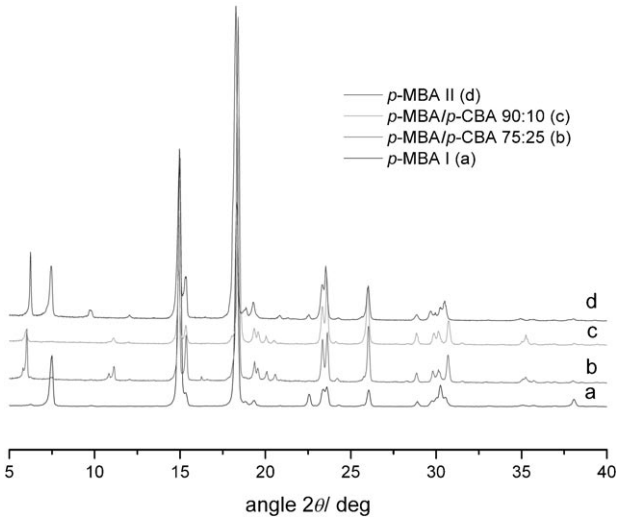


Figure 10. X-ray powder patterns of form *p*-MeBA I and form *p*-MeBa II compared with X-ray powder patterns of *p*-ClBA/*p*-MeBA in 10:90 and 25:75 molar ratios.

Crystallization from solution of the mixture *p*-ClBA/*p*-MeBA 10:90 allowed the formation of single crystals of appropriate size for X-ray diffraction. The structure was solved in a monoclinic system with space group $P2_1/c$ (see Table 2 for details) with two independent molecules in the asymmetric unit ($Z=2$). As in the other phases the hydroxyl group is involved in hydrogen-bond interactions creating infinite chains, packed in an anti-parallel fashion (Figure 11).

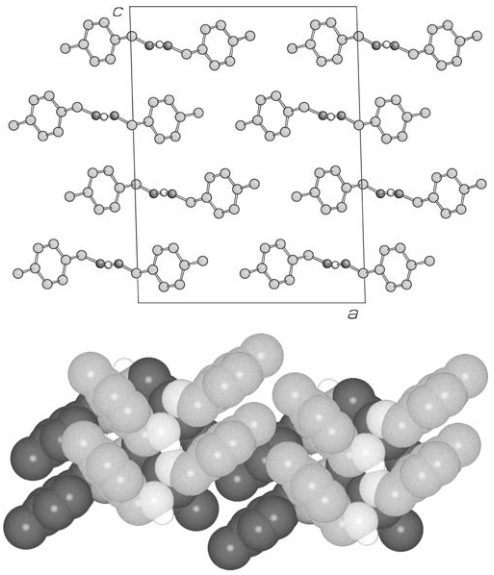


Figure 11. View of the crystal packing of the *p*-ClBA/*p*-MeBA 10:90 structure along the *b* axis (top) and view of the different orientation of the chains along the *c* axis (bottom). Only one image of disorder and no $H_{CH}$ atoms are shown for clarity.

## Conclusion

With this paper we have provided further evidence that the hetero-seeding method can be a successful route to obtaining new crystal forms. In the case of *p*-MeBA II, the commercial form of *para*-methylbenzyl alcohol, the traditional polymorph screening does not seem to yield any alternative crystal packing. A new crystal of *p*-MeBA (*p*-MeBA I) isomorphic to the commercial *p*-ClBA has been obtained for the first time by hetero-seeding of a supersaturated solution with crystals of *p*-ClBA. The new form has been fully characterized by X-ray single-crystal diffraction, calorimetry experiments, and SSNMR spectroscopy. The different aromatic CH environments displayed by the two phases are clearly detected by $^{13}C$ CPMAS spectra. The two polymorphs can be described as a monotropic system in which form II is the thermodynamically stable form and form I is the metastable form. Furthermore, the infinitive miscibility of the two isomorphous compounds *p*-MeBA I and *p*-ClBA has been exploited in the preparation of mixed crystals, whereby the Me group and the Cl atom are statistically disordered in the crystal. The solid solutions quenched in liquid nitrogen with a molar ratio *p*-ClBA/*p*-MeBA 10:90 and 25:75 produce a new phase. In all the structures the hydrogen-bond pattern is maintained and the difference arises in the packing of the infinite chains. This difference involves mainly van der Waals interactions and does not seem to affect the overall architecture, resulting in quite similar powder patterns although the cell parameters are clearly different and do not interconvert.

## Experimental Section

**Solvent screening**: *p*-ClBA (80 mg) was dissolved in different solvents (2.5–3.5 mL; water, ethanol, isopropyl alcohol, acetone, ethyllactate, dioxane, hexane, toluene, nitromethane, THF, (*S*)-methylbuthanol, dichloromethane, THF/$H_2O$, hexane/diethyl ether). The limpid solutions were allowed to evaporate at RT. The crystals recovered were characterized by XRPD. In all cases the *p*-ClBA form was observed.

*p*-MeBA (100 mg) was dissolved in different solvents (2.5–3.5 mL; water, ethanol, acetone, ethyllactate, dioxane, hexane, toluene, nitromethane, (*S*)-methylbutanol). The limpid solutions were allowed to evaporate at RT. The crystals recovered were characterized by XRPD. In all cases *p*-MeBA form II was observed.

**Supersaturation and evaluation of the metastable zone**: *p*-ClBA (400 mg) was added to hexane (3 mL) and the slurry was stirred at RT for 1 h without complete dissolution. Complete dissolution was obtained at 55 °C. However, the solution was heated up to 70 °C, and it was allowed to cool slowly without stirring; the first visible crystals appeared at 42 °C. The crystals obtained were filtered and characterized as the known form of *p*-ClBA. The metastable zone was considered between 49 and 53 °C.

*p*-MeBA (500 mg) was added to hexane (3 mL) and the slurry was stirred at RT for 1 h without complete dissolution. Complete dissolution was obtained at 43 °C. However, the solution was heated up to 60 °C and was allowed to cool slowly without stirring; the first visible crystals appeared at

  

33 °C. The crystals obtained were filtered and characterized as the known form II of *p*-MeBA. The metastable zone was considered between 37 and 41 °C.

**Sublimation**: *p*-ClBA (150 mg) was sublimed at 60 °C under vacuum and condensed on a cold finger at 0 °C. The known form was recovered.

*p*-MeBA (150 mg) was sublimed at 45 °C under vacuum and condensed on a cold finger at 0 °C. Form II was recovered.

**Melting**: *p*-ClBA (100 mg) was melted and allowed to cool slowly at RT or quenched at 0 °C or −196 °C. In all cases the XRPD pattern corresponded to the known form.

*p*-MeBA (100 mg) was melted and allowed to cool slowly at RT or quenched at 0 °C or −196 °C. In all cases the XRPD pattern corresponded to form II.

**Hetero-seeding**: *p*-ClBA (400 mg) was added to hexane (3 mL) and the slurry was heated up to 70 °C. The limpid solution obtained was allowed to cool without stirring, and at 50 °C crystalline powder (10 mg) and a couple of crystals (1×1×0.3 mm) of *p*-MeBA II were added to the solution. These crystals rapidly dissolved without starting the crystallization. The crystals finally obtained were characteristic of the known phase of *p*-ClBA.

*p*-MeBA (500 mg) was added to hexane (3 mL) and the slurry was heated up to 60 °C. The limpid solution obtained was allowed to cool without stirring. At 38 °C two single crystals of *p*-ClBA were added to the solution, and immediate formation of crystals was observed, which were characterized as form I of *p*-MeBA.

**Homo-seeding**: *p*-MeBA (500 mg) was added to hexane (3 mL) and the slurry was heated up to 60 °C. The limpid solution obtained was allowed to cool without stirring. At 38 °C *p*-MeBA I (10 mg) was added to the solution, and immediate formation of crystals of *p*-MeBA was observed, which were characterized as form I of *p*-MeBA.

**Solid mixtures**: *p*-MeBA II (61 mg, 0.5 mmol) was ground and added to ground *p*-ClBA (71 mg, 0.5 mmol). The mixture was homogenized and the XRPD shows the pattern of the two phases, and DSC shows the melting point of the eutectic at 51.4 °C.

*p*-MeBA I (61 mg, 0.5 mmol) was ground and added to ground *p*-ClBA (71 mg, 0.5 mmol). The mixture was homogenized; the XRPD shows the pattern of the two phases, and DSC shows the melting point of the eutectic at 51.1 °C.

*p*-MeBA II (30.5 mg, 0.25 mmol) was ground and added to ground *p*-ClBA (106.5 mg, 0.75 mmol). The mixture was homogenized and the XRPD shows the pattern of the two phases, while the DSC shows the melting point of the eutectic at 50.8 °C followed by melting of *p*-ClBA at 62–65 °C. In a second heating only one endothermic peak is observed with its onset at 55.0 °C, which is consistent with the presence of a solid solution.

*p*-MeBA II (91.5 mg, 0.75 mmol) was ground and added to ground *p*-ClBA (35.5 mg, 0.25 mmol). The mixture was homogenized; the XRPD shows the pattern of the two phases, and the DSC shows the melting point of the eutectic at 51.9 °C.

**Solid solutions**: Solid solutions were obtained by melting together *p*-ClBA and *p*-MeBA II in 10:90, 25:75, 50:50, 75:25, and 90:10 molar ratios. The melts were quenched in ice or liquid nitrogen. In all cases only one phase was obtained and was characterized by XRPD and DSC. *p*-ClBA, phase I, m.p. 70.4 °C; *p*-ClBA/*p*-MeBA 90:10, phase I, m.p. 63.6 °C; *p*-ClBA/*p*-MeBA 75:25, phase I, m.p. 52.9 °C; *p*-ClBA/*p*-MeBA 50:50, phase I, m.p. 51.6 °C; *p*-ClBA/*p*-MeBA 25:75, phase new, m.p. 54.8 °C; *p*-ClBA/*p*-MeBA 10:90, phase new, m.p. 52.9 °C; *p*-MeBA, phase II, m.p. 58.0 °C.

A mixture of *p*-ClBA/*p*-MeBA (500 mg) in the molar ratio 40:60 were added to hexane (3 mL) and the slurry was heated up to 70 °C. The limpid solution obtained was allowed to cool without stirring, and at 50 °C a few crystals of *p*-ClBA were added to the solution. Immediate formation of crystals followed, which were characterized as *p*-ClBA/*p*-MeBA 40:60 form I.

**DSC measurements**: Calorimetric measurements were performed by using a Perkin–Elmer Diamond equipped with a model ULSP90 intracooler. Temperature and enthalpy calibrations were performed by using high purity standards (*n*-decane, benzene and indium). The samples (3–5 mg) were placed in aluminum open pans. Heating was carried out at 5 °C min$^{-1}$ in the temperature range from 25 to 100 °C.

**SSNMR**: Solid-state NMR measurements were run on a Bruker AVANCE II 400 instrument operating at 400.23 and 100.65 MHz for $^{1}$H and $^{13}$C, respectively. All spectra were recorded at room temperature at the spinning speed of 12 kHz. Cylindrical 4 mm o.d. zirconia rotors with sample volume of 120 mL were employed. A ramp cross-polarization pulse sequence was used with a contact time of 3 ms ($^{13}$C), a $^{1}$H 90° pulse of 3.35 ms, recycle delays of 5–15 s, and 600–2000 transients. A two pulse phase-modulation (TPPM) decoupling Scheme was used with a frequency field of 75 kHz.

**X-ray powder diffraction**: X-ray powder diffraction patterns were collected on a Panalytical X'Pert PRO automated diffractometer with $Cu_{K\alpha}$ radiation and an X'Celerator detector without a monochromator. When required, powder data were collected with a spinner capillary stage to decrease the preferential orientation effect. The program PowderCell[47] was used for calculation of X-ray powder patterns.

**Crystal structure determination**: Crystal data for *p*-ClBA/*p*-MeBA 10:90 were collected on a Nonius CAD4 diffractometer; crystal data for *p*-

Table 2. Crystal data and details of measurements for *p*-MeBA I and *p*-ClBA/*p*-MeBA 10:90.

| | *p*-MeBA I | *p*-ClBA/*p*-MeBA 40:60 | *p*-ClBA/*p*-MeBA 40:60 | *p*-ClBA/*p*-MeBA 10:90 |
|---|---|---|---|---|
| formula | $C_8H_{10}O_1$ | $C_{7.60}H_{8.80}Cl_{0.40}O_1$ | $C_{7.60}H_{8.80}Cl_{0.40}O_1$ | $C_{7.90}H_{9.70}Cl_{0.10}O_1$ |
| $M_r$ | 122.16 | 130.33 | 130.33 | 124.20 |
| system | monoclinic | monoclinic | monoclinic | monoclinic |
| space group | $P2_1$ | $P2_1$ | $P2_1$ | $P2_1/c$ |
| $T$ [K] | 298 | 298 | 150 | 298 |
| $a$ [Å] | 12.112(1) | 12.159(1) | 12.1927(11) | 14.686(3) |
| $b$ [Å] | 4.9803(5) | 4.9749(7) | 4.8676(3) | 4.957(2) |
| $c$ [Å] | 6.0018(6) | 5.9592(9) | 5.8625(5) | 19.231(4) |
| $\beta$ [°] | 102.691(1) | 103.75 (1) | 103.804(9) | 91.67(2) |
| $V$ [Å$^3$] | 353.19(6) | 350.14(8) | 337.89(5) | 1399.4(7) |
| $Z$ | 2 | 2 | 2 | 8 |
| $\mu(Mo_{K\alpha})$ [mm$^{-1}$] | 0.074 | 0.227 | 0.235 | 0.113 |
| measured reflns | 2801 | 1970 | 1367 | 2536 |
| unique reflns | 1451 | 1273 | 1110 | 2452 |
| refined parameters | 76 | 97 | 96 | 149 |
| GOF on $F^2$ | 1.088 | 1.107 | 1.054 | 0.924 |
| $R1$ [on $F$, $I>2\sigma(I)$] | 0.0630 | 0.0447 | 0.0407 | 0.0633 |
| $wR2$ (on $F^2$, all data) | 0.1894 | 0.1195 | 0.1021 | 0.3015 |

MeBA I were collected on a Bruker Smart Apex II CCD; crystal data for *p*-ClBA/*p*-MeBA 40:60 at RT and −123 °C were collected on an Oxford Xcalibur S equipped with a liquid nitrogen Oxford-Cryostream device. Crystal data and details of measurements are summarized in Table 2. Common to all compounds: $Mo_{K\alpha}$ radiation, $\lambda = 0.71073$ Å, monochromator graphite. SHELX97[48] was used for structure solution and refinement based on $F^2$. Non-hydrogen atoms were refined anisotropically. Hydrogen atoms bound to carbon atoms were added in calculated positions. In the crystal structure of *p*-ClBA/*p*-MeBA 10:90 methyl and chlorine groups were disordered and the occupancies were refined as Cl:Me 10:90. In the crystal structure *p*-ClBA/*p*-MeBA 40:60 methyl and chlorine groups were disordered and the occupancies were refined as Cl:Me 40:60. SCHAKAL[49] was used for the graphical representation of the results. The program PLATON[50] was used to calculate the hydrogen bonding interactions. CCDC-677231, -677232, and -692381, and -692382 contain the supplementary crystallographic data for this paper. These data can be obtained free of charge from The Cambridge Crystallographic Data Centre via www.ccdc.cam.ac.uk/data_request/cif.

## Acknowledgements

We acknowledge financial support from MIUR and the University of Bologna. The participation of the undergraduate student Salvatore Portas in the crystallization experiments is gratefully acknowledged.

[1] J. Bernstein, *Polymorphism in Molecular Crystals*, Oxford University Press, Oxford, **2002**, p. 352.
[2] H. G. Brittain, *Polymorphism in Pharmaceutical Solids*, Marcel Dekker, New York, **1999**, p. 427.
[3] R. Hilfiker, *Polymorphism*, Wiley VCH, Weinheim, **2006**.
[4] J. J. Novoa, D. Braga, L. Addadi, *Engineering of Crystalline Materials Properties*, Springer, Dordrecht, **2008**, pp. 1–518.
[5] S. L. Morissette, O. Almarsson, M. L. Peterson, J. F. Remenar, M. J. Read, A. V. Lemmo, S. Ellis, M. J. Cima, C. R. Gardner, *Adv. Drug Delivery Rev.* **2004**, *56*, 275–300.
[6] C. P. Price, A. L. Grzesiak, A. J. Matzger, *J. Am. Chem. Soc.* **2005**, *127*, 5512–5517.
[7] C. Cashell, D. Corcoran, B. K. Hodnett, *Cryst. Growth Des.* **2005**, *5*, 593–597.
[8] N. Blagden, *Powder Technol.* **2001**, *121*, 46–52.
[9] X. He, J. G. Stowell, K. R. Morris, R. R. Pfeiffer, H. Li, G. P. Stahly, S. R. Byrn, *Cryst. Growth Des.* **2001**, *1*, 305–312.
[10] D. Braga, M. Cadoni, F. Grepioni, L. Maini, K. Rubini, *CrystEngComm* **2006**, *8*, 756–763.
[11] D. Braga, M. Curzi, F. Grepioni, M. Polito, *Chem. Commun.* **2005**, 2915–2917.
[12] A. V. Trask, N. Shan, W. D. S. Motherwell, W. Jones, S. Feng, R. B. H. Tan, K. J. Carpenter, *Chem. Commun.* **2005**, 880–882.
[13] A. V. Trask, J. van de Streek, W. D. S. Motherwell, W. Jones, *Cryst. Growth Des.* **2005**, *5*, 2233–2241.
[14] H. Shinozaki, T. Oguchi, S. Suzuki, K. Aoki, T. Sako, S. Morishita, Y. Tozuka, K. Moribe, K. Yamamoto, *Drug Dev. Ind. Pharm.* **2006**, *32*, 877–891.
[15] I. Pasquali, R. Bettini, F. Giordano, *Eur. J. Pharm. Sci.* **2006**, *27*, 299–310.
[16] F. P. A. Fabbiani, C. R. Pulham, *Chem. Soc. Rev.* **2006**, *35*, 932–942.
[17] F. P. A. Fabbiani, D. R. Allan, W. G. Marshall, S. Parsons, C. R. Pulham, R. I. Smith, *J. Cryst. Growth* **2005**, *275*, 185–192.
[18] M. Bujak, A. Budzianowski, A. Katrusiak, *Z. Kristallogr.* **2004**, *219*, 573–579.
[19] D. Braga, G. Cojazzi, D. Paolucci, F. Grepioni, *CrystEngComm* **2001**, *3*, 159–161.
[20] H. Miura, T. Ushio, K. Nagai, D. Fujimoto, Z. Lepp, H. Takahashi, R. Tamura, *Cryst. Growth Des.* **2003**, *3*, 959–965.
[21] A. I. Kitaigorodskii, *Molecular Crystals and Molecules*, Academic Press, New York, **1973**, p. 553.
[22] G. R. Desiraju, J. A. R. P. Sarma, *Proc. Indian Acad. Sci.* **1986**, *96*, 599.
[23] N. N. Laxmi Madhavi, A. K. Katz, H. L. Carrell, A. Nangia, G. R. Desiraju, *Chem. Commun.* **1997**, 1953–1954.
[24] W. Jones, C. R. Theocharis, J. M. Thomas, G. R. Desiraju, *J. Chem. Soc. Chem. Commun.* **1983**, 1443–1444.
[25] L. Sacconi, M. Ciampolini, G. P. Speroni, *J. Am. Chem. Soc.* **1965**, *87*, 3102–3106.
[26] M. R. Edwards, W. Jones, W. D. S. Motherwell, *CrystEngComm* **2006**, *8*, 545–551.
[27] G. R. Desiraju, R. Parthasarathy, *J. Am. Chem. Soc.* **1989**, *111*, 8725–8726.
[28] A. Gavezzotti, *Molecular Aggregation*, Oxford University Press, **2006**, p. 384.
[29] C. M. Reddy, M. T. Kirchner, R. C. Gundakaram, K. A. Padmanabhan, G. R. Desiraju, *Chem. Eur. J.* **2006**, *12*, 2222–2234.
[30] I. Csöregh, T. Brehmer, P. Bombicz, E. Weber, *Cryst. Eng.* **2001**, *4*, 343–357.
[31] M. Hashimoto, M. Harada, *Z. Naturforsch. A* **2003**, *58*, 63–67.
[32] M. Hashimoto, Y. Nakamura, K. Hamada, *Acta Crystallogr. Sect. C* **1988**, *44*, 482–484.
[33] M. Hashimoto, M. Harada, M. Mizuno, M. Hamada, T. Ida, M. Suhara, *Z. Naturforsch. A* **2002**, *57*, 381–387.
[34] J. W. Steed, *CrystEngComm* **2003**, *5*, 169–179.
[35] K. M. Anderson, J. W. Steed, *CrystEngComm* **2007**, *9*, 328–330.
[36] G. R. Desiraju, *CrystEngComm* **2007**, *9*, 91–92.
[37] A. Nangia, *Acc. Chem. Res.* **2008**, *41*, 595–604.
[38] A. Gavezzotti, *CrystEngComm* **2008**, *10*, 389–398.
[39] M. R. Chierotti, R. Gobetto, *Chem.Commun.* **2008**, 1621–1634.
[40] D. Braga, S. L. Giaffreda, K. Rubini, F. Grepioni, M. R. Chierotti, R. Gobetto, *CrystEngComm* **2007**, *9*, 39–45.
[41] D. Braga, S. L. Giaffreda, F. Grepioni, M. R. Chierotti, R. Gobetto, G. Palladino, M. Polito, *CrystEngComm* **2007**, *9*, 879–881.
[42] D. E. B. S. R. B. Patrick A. Tishmack, *J. Pharm. Sci.* **2003**, *92*, 441–474.
[43] D. Braga, L. Maini, C. Fagnano, P. Taddei, M. R. Chierotti, R. Gobetto, *Chem. Eur. J.* **2007**, *13*, 1222–1230.
[44] R. Gobetto, C. Nervi, M. R. Chierotti, D. Braga, L. Maini, F. Grepioni, R. K. Harris, P. Hodgkinson, *Chem. Eur. J.* **2005**, *11*, 7461–7471.
[45] M. Nishio, *CrystEngComm* **2004**, *6*, 130–158.
[46] W. I. F. David, K. Shankland, J. van de Streek, E. Pidcock, W. D. S. Motherwell, J. C. Cole, *J. Appl. Crystallogr.* **2006**, *39*, 910–915.
[47] W. Kraus, G. Nolze in *Powder Cell, Vol.* **1999**.
[48] G. M. Sheldrick, SHELXL97, **1997**, University of Göttingen, Göttingen (Germany).
[49] E. Keller, **1999**, SCHAKAL99, Graphical Representation of Molecular Models, University of Freiburg, Freiburg (Germany).
[50] A. L. Spek, *Acta Crystallogr. Sect. A* **1990**, *46*, C34.

Received: March 3, 2008
Revised: September 9, 2008
Published online: December 29, 2008

  